

NASA CR- 166795

ION DRIFT METER

FOR

DYNAMICS EXPLORER

FINAL REPORT

For Contract No. NAS5-24297

TO

NATIONAL AERONAUTICS AND SPACE ADMINISTRATION

GODDARD SPACE FLIGHT CENTER

FROM

THE UNIVERSITY OF TEXAS AT DALLAS

CENTER FOR SPACE SCIENCES

(NASA-CR-166795) ION DRIFT METER FOR  
DYNAMICS EXPLORER Final Report (Texas  
Univ.) 33 p HC A03/MF A01 CSCL 14B

N82-25318

Unclas  
G3/19 21922

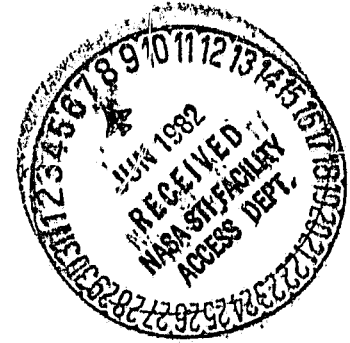
R. A. Heelis  
Principal Investigator

W. B. Hanson  
Co-Investigator

C. R. Lippincott  
Co-Investigator

D. R. Zuccaro  
Co-Investigator

FEBRUARY 1982



FINAL REPORT  
CONTRACT NO. NAS5-24297  
ION DRIFT METER  
FOR  
DYNAMICS EXPLORER

SUMMARY

The Ion Drift Meter (IDM) on the Dynamics Explorer B (DE-B) satellite was launched on August 3, 1981, 0956 UT from the Western Test Range. Since turn-on of the instrument, it has performed well and data reduction and analysis have started. Any anomalous instrument operation can be worked around or does not appear to adversely affect the data gathering or analysis of the instrument. Long-term data analysis and scientific results will be reported through publication in the appropriate scientific journals. That effort is funded under a separate contract (NAS5-26068) between the University of Texas at Dallas and Goddard Space Flight Center. Other final reports (such as New Technology and equipment) for the hardware contract have been submitted per the contract under separate cover. Also it should be pointed out that all instrument design reviews were completed satisfactorily and all resulting action items closed. Design review data packages were delivered under separate cover at the appropriate time.

The objective of the investigation is to provide a better understanding of the plasma dynamics in the magnetosphere. In particular the instrument will measure the components of the thermal ion bulk velocity perpendicular to the satellite velocity vector. These measurements will be of value in quantifying the polar and auroral convective pattern, the refilling of the

plasmasphere after a magnetic storm, and in determining the extent of interhemisphere plasma flow. The particular measurements used here are based on a technique tested and proven on Atmosphere Explorer. Unfortunately the complementary measurements with magnetometers and electric field antennae (both AC and DC measurements) necessary to unravel the complete plasma behavior were not made on Atmosphere Explorer, nor were conditions sampled far into the magnetosphere. These factors, plus the cooperative use of the upper and lower DE satellites, add whole new dimensions to the usefulness of the measurements.

The investigation entails the in-situ measurement of the bulk motion of the thermal ions. These data, in conjunction with other measurements that will be carried out in the mission, will be extremely useful in our attempt to understand the coupling between the solar wind and the lower ionosphere and atmosphere.

It is anticipated that these measurements will yield valuable information on:

- a) the ion convection (electric field) pattern in the auroral and polar ionosphere.
- b) the flow ions along magnetic field lines within the plasmasphere, whether this motion is simply a breathing of the protonosphere, a refilling of this region after a storm, or an interhemisphere transport of plasma.
- c) velocity fields associated with small scale phenomena that are important at both low and high latitudes.

The detailed instrument parameters and investigative approach are presented in the following paper.

THE ION DRIFT METER FOR DYNAMICS EXPLORER-B

by

R. A. Heelis, W. B. Hanson  
C. R. Lippincott, D. R. Zuccaro, L. H. Harmon,  
B. J. Holt, J. E. Doherty and R. A. Power

Center for Space Sciences, Physics Program  
The University of Texas at Dallas  
Richardson, TX 75080

Accepted by

Space Science Instrumentation

September 1981

## Abstract

The ion drift meter for Dynamics Explorer B measures two mutually perpendicular angles of arrival of thermal ions with respect to the sensor look directions. These angles lie in the vertical and horizontal planes and may be thought of as pitch and yaw in the conventional aerodynamic sense. The components of the ion drift velocity along vertical and horizontal axes through the spacecraft body are derived to first order from knowledge of the spacecraft velocity vector and more accurately with additional knowledge of the component of ion drift along the sensor look direction.

## INTRODUCTION

An overview of the Dynamics Explorer program is given by Hoffman and Schmerling.[1] Fulfillment of many of the scientific objectives of this mission require a knowledge of the motion of the ionospheric plasma. Motion of the ionospheric ions is important both to their distribution, composition and temperature.[2] Rapid motion affects the ion temperature by Joule heating and the ion composition by the dependence of chemical time constants on the ion energy. Convective motion of the ions can transport high concentrations of ions from the dayside to the nightside of the high latitude ionosphere and significantly affect the concentrations that might be expected from simple solar and particle production. Motion of the ions parallel to the earth's magnetic field may in some cases constitute a net current while in others it may constitute a method of storing plasma during the day.[3]

The component of the ion motion perpendicular to the earth's magnetic field is of course derivable from an electric and magnetic field measurement. However, parallel to the magnetic field, the electrostatic field and the ion drift velocity are not simply related and constitute quite different geophysical parameters. Measurement of the ion drift velocity vector is made by the Retarding Potential Analyzer (RPA) and the Ion Drift Meter (IDM) on DE-B. These instruments are mounted so that they look along the spacecraft X axis, and figure 1a) shows the relationship between the direction of the incoming ions with respect to the spacecraft and the spacecraft axes X, Y and Z. In the spacecraft frame the ion velocity  $\underline{v}$  is made up of the ambient ion velocity  $\underline{v}^i$  and the spacecraft velocity  $\underline{v}^s$ . The velocity com-

ponents parallel and perpendicular to the sensor look direction  $V_{||}$  and  $V_{\perp}$  are determined by the RPA and IDM respectively. The RPA is described in detail by Hanson et al.[4]. The ion velocity perpendicular to the sensor look direction is made up of two components along the Y and Z axes of the spacecraft. Figure 1b) shows a projection onto the XZ plane of the situation in figure 1a) and illustrates the relationship

$$-V_Z^S + V_Z^i = (-V_X^S + V_X^i) \tan \alpha = V_{||} \tan \alpha$$

that is used to determine  $V_Z^i$ . A similar relationship between  $V_Y^i \tan \beta$  and  $V_{||}$  is used to determine  $V_Y^i$ . The segmented collector shown in figure 1b) illustrates that a natural asymmetry in the current to opposite collector segments results if  $\alpha$  is non zero. Since the ion current to the collector is proportional to the irradiated area it can be shown that the ratio R of currents to each collector pair is given by

$$R = \frac{W/2 + D \tan \alpha}{W/2 - D \tan \alpha}$$

The IDM determines the current ratio R to measure the arrival angle  $\alpha$ . By utilizing 4 collector segments connected in pairs a similar geometry in the XY plane can be established and the angle  $\beta$  can be determined. It can be seen that the spacecraft velocity along the X, Y and Z axes as well as the ambient ion drift velocity along the X axis is required to determine  $V_Y$  and  $V_Z$  from  $\alpha$  and  $\beta$ . Thus, knowledge of the spacecraft attitude and the RPA derived component of ion velocity is required to produce  $V_Y$  and  $V_Z$  with their smallest error.

## INSTRUMENTATION

The IDM for DE-B is very similar in design to those used successfully on the AE satellites.[5] A sensor consists of a square entrance aperture that serves as a collimator, some electrically isolating grids and a segmented planar collector. The angle of arrival of the ions with respect to the sensor is determined by measuring the ratio of the currents to the different collector segments. This ratio is determined by taking the difference in the logarithms of the current. We use two techniques to determine this ratio. In the first, called the standard drift sensor (SDS), the collector segments are connected in pairs to two logarithmic amplifiers. These log amplifiers provide the inputs to a single linear difference amplifier that measures either a horizontal arrival angle or the vertical arrival angle. The logarithmic amplifiers have a 5 decade dynamic range measuring currents from  $10^{-11}$  amps to  $10^{-6}$  amps. The linear difference amplifier has three sensitivity ranges with sensitivities successively differing by a factor of 4, which provides a total dynamic range equivalent to about plus to minus 50 degrees in ion arrival angle. This technique is described in detail by Hanson and Heelis.[6] It has the advantage that absolute differences between the log electrometers can be eliminated by a rezeroing technique, but a disadvantage that the horizontal and vertical arrival angles cannot be determined simultaneously. In addition, this technique involves some switching at the collectors themselves and thus the collectors are maintained at ground potential to minimize the effects of electrical transients.

The desire to perform the horizontal and vertical measurements simultaneously and to have the ability to bias the collector above and below ground potential in order to investigate other instrument characteristics led to the design of an alternative technique called the universal drift sensor (UDS).



With this technique each collector segment is permanently connected to a logarithmic amplifier and two difference amplifiers are used to determine the horizontal and vertical arrival angles simultaneously. The logarithmic amplifiers are identical to those used in the SDS. The difference amplifiers have four ranges each different by  $\sqrt{10}$  so that a total dynamic range equivalent to about plus to minus 50 degrees in ion arrival angle is again available. The UDS advantage of simultaneity in angle measurements is compromised by the fact that absolute differences between the electrometers cannot be eliminated from the difference amplifier output. The IDM consists of two sensors - one providing the SDS output and the other providing the UDS output. Each sensor is provided with 4 main frame telemetry words for analog signals and a digital word providing range and instrument function information. For each sensor the difference amplifier output is telemetered as the primary signal that is almost directly proportional to the ion arrival angle. Sampling of this output is preceded by a sequence of operations that are synchronized to the telemetry and are different for the SDS and the UDS.

Mechanically, the size and grid arrangements for the two sensors are identical and are shown in cross-section in figure 2. The entrance apertures are covered by double grids,  $G_1$ , that are grounded and surrounded by a flat gold plated ground plane to ensure that transverse electric fields are minimized inside and outside the sensor. The grid  $G_2$  is always grounded in the SDS to provide a field free drift space inside the instrument. In the UDS different potentials are applied to this grid to investigate the effects of spurious currents that will be described later. The instrument sensitivity can be drastically changed when hydrogen ions are present, since their random thermal velocity is comparable to the spacecraft velocity.[6] While correction for this sensitivity change can be made,  $O^+$  ions are almost always present to allow a signal from ions whose random thermal velocity is

much smaller than the spacecraft velocity. Thus grid  $G_3$  may be biased at a small positive potential to prevent hydrogen ions from striking the collector. Grid  $G_4$  is always biased at  $-15V$  to prevent thermal electrons from striking the collector and to suppress photo-emission from the collector. The collector itself is grounded in the SDS, whereas in the UDS it is biased at  $-2 V$  or  $+17 V$ , depending on its mode of operation. A summary of the instrument's characteristics and functions is given in Table 1.

#### SDS Operation

As was pointed out earlier, the SDS has the advantage that absolute differences between the logarithmic amplifiers can be removed from the arrival angle determination. These differences are removed by performing a "rezero" and "offset" sequence. During a "rezero" operation the output of the difference amplifier is stored in a capacitor and this value is set to the middle of the telemetry band ( $2.5 V$ ) to ensure maximum sensitivity to subsequent deviations of either sign. The inputs to the logarithmic amplifiers are then interchanged and the difference amplifier output relative to the capacitor value is telemetered. Thus a value equal to twice the absolute "offset" between the two logarithmic amplifiers is telemetered. Following this offset operation the original logarithmic amplifier inputs are re-established and values relative to the rezero value are telemetered until the sequence is repeated. During the rezero and offset sequences the difference amplifier input passes through a 3 pole Bessel filter that is 3 dB down at 270 Hz to lessen the effects of switching transients. Subsequently a slower filter that is 3 dB down at 27 Hz is used to prevent aliasing at the sample rate. Ground commands are used to determine if the rezero and offset sequence occupies  $1/8$  second or  $1/16$  second and to set the repeat frequency for rezero and offset sequences to  $1/8$  second or 8 seconds.

During these operations any one of 16 positive bias voltages between 0 to +3.75 V in 0.25 volt increments can be selected by ground command and applied to grid  $G_3$  to prevent  $H^+$  ions from striking the collector. In general this grid will either be grounded or have the minimum voltage necessary to retard  $H^+$  ions applied to it. In addition, ground commands are available so that the collector configuration for rezero and offset sequences and subsequent relative arrival angles may alternate between horizontal and vertical angles or be fixed on either one. If the rezero and offset sequence is repeated only every 8 seconds there is a substantial period during which there is no collector or electronic switching, and the absence of transients from these operations makes the data amenable to power spectral analysis. The RPA has associated with it a series of 6 filters covering the range 64 Hz to 8.5 KHz in factors of e, and it will be possible to share the lower 5 of these filters between the total ion current measured by the RPA and the horizontal or vertical arrival angle measured by the SDS. Thus a measure of the small-scale structure in the velocity will be available. Details of the filter bank are described more fully by Hanson et al.[4]

#### UDS Operation

For this sensor great care has been taken to remove any offsets between the logarithmic amplifiers that might be interpreted as ambient ion drifts. Nevertheless, precautions must be taken to ensure that such offsets do not adversely affect the signal and prevent us from making use of the instrument sensitivity. In order to ensure such sensitivity the difference amplifier output is periodically grounded through a capacitor and the telemetry output is set to the middle of the telemetry band. Subsequently the difference amplifier output is monitored relative to the newly established "zero" on

the capacitor and with maximum sensitivity to deviations of either sign. During this zero operation the absolute output of each logarithmic amplifier is also telemetered. The "zero" operation occupies 1/16 second and is repeated every 8 seconds. Since only single collector segments supply the inputs to the difference amplifiers, there are always two collector pairs that provide horizontal or vertical arrival angles. The UDS provides automatic selection of a collector segment pair for a given arrival angle direction by determining the collector segment with the largest current and selecting it and the appropriate adjacent quadrant. The capability also exists to override the automatic collector selection in case of failure and to determine the characteristics of all the logarithmic amplifiers. It is, therefore, possible to select a given collector segment and the appropriate adjacent quadrant by ground command. Ground commands are also used to enable each difference amplifier to be configured for horizontal ion arrival angles only, vertical ion arrival angles only or alternate between horizontal and vertical at the "zero" sequence repeat rate (8 seconds). As with the SDS any one of 16 positive bias voltages between 0 and +3.75 V in 0.25 V increments can be selected by ground command and applied to the repeller grid  $G_3$  to prevent  $H^+$  ions from striking the collector.

It has been well established in data from the Atmosphere Explorer satellites that neutral particle impacts on the drift meter collectors can produce ion emission that can distort the output signal and in some cases completely dominate the ambient ion current.[4] These net negative currents can be measured with the UDS. Here the shield grid  $G_2$  is biased at +15 V to prevent ambient ions from striking the collector. The collector is biased at +17 V to ensure that any ions leaving the collector can overcome the +15 V shield grid potential and not return to the collector,

and the suppressor grid is maintained at -15 volts. In this configuration we are able to measure the absolute ion currents produced by neutral particle impact. In addition, if the ion emission from the collectors is uniform across the collector surface, the difference amplifier output should be proportional to the neutral particle arrival angle and hence to the transverse neutral drift velocity. While we have limited confidence that this mode will produce geophysical data, it might provide excellent data concerning the nature of these background currents.

Negative collector currents also result from energetic electrons and photoelectrons that strike the collectors. We are able to assess the effect of these signals on our data by using the previous grid voltage configuration except that the collector is biased at -2 V to suppress the liberation of ions discussed above.

In all the above functions the 8 sec cycle time described at the beginning of the UDS description is preserved. However, in recognition of the fact that there is a possibility of providing neutral particle drift data, a mode is also included that allows the UDS to alternate between ambient ion measurements and neutral particle measurements every 1/4 second.

In principle the UDS is capable of providing simultaneous horizontal and vertical ion arrival angle data, although the technique has not been tried before. In the unlikely event that this proves to be superior to the SDS sensor or that the SDS sensor should fail, we have the capability to assign all the telemetry to the UDS by ground command. In this mode we can regain the 1/64 sec resolution on simultaneous measurements available from operating the UDS and SDS in tandem.

TABLE I: INSTRUMENT SUMMARY

Weight	Electronics Box	2.20 kg
	Sensors	<u>1.70</u> kg
	TOTAL	3.90 kg
Power		3.5 watts
Telemetry		1.28 kbps

<u>Grid Biases</u>	<u>SDS</u>	<u>UDS</u>		
		<u>Ions</u>	<u>Neutrals</u>	<u>Electrons</u>
Collector	0	-2	+17	-2
Suppressor G <sub>4</sub>	-15	-15	-15	-15
Repeller G <sub>3</sub>	0-3.75	0-3.75	0-3.75	0-3.75
Shield G <sub>2</sub>	0	0	+15	+15
Input G <sub>1</sub>	0	0	0	0

Geophysical Parameters	<u>Range</u>	<u>Accuracy</u>	<u>Nominal Resolution</u>
Transverse Horizontal ion drift	-4 km/sec to + 4 km/sec	<u>+ 50 m/sec*</u>	1/32 sec
Transverse Vertical ion drift	-4 km/sec to + 4 km/sec	<u>+ 50 m/sec</u>	1/32 sec

\*The instrument sensitivity is about 3 m/sec and an accuracy of 50 m/sec is determined from the expected accuracy in vehicle attitude determination of about 0.5 degrees.

## DATA PRESENTATION

Routine data processing for both UDS and SDS will be performed by programs run on the Science Data Processing System. Microfilm/microfiche displays will be the primary source of visual data; Figure 3 shows a typical microfilm display. The data will initially be converted from arrival angle to drift velocity assuming the ram component of drift from the RPA is zero. In general the X component of the spacecraft velocity will be much larger than the same component of the ambient ion drift velocity and the error in the derived velocity components along the Y and Z axes will be quite small. The data are plotted independently for the UDS and the SDS and a 20 minute frame will contain data points every 1/4 sec. The data will be stored at this time base in the Mission Analysis Files (MAF's). In addition, when data are available at higher time resolution additional plot frames will be produced in 1 minute frames. These high resolution data will not be stored in MAF's. The display will show one or two velocity components for SDS depending upon the instrument mode and differentiated by different line patterns. In addition the components of the spacecraft velocity relative to a corotating atmosphere along the two transverse axes Y and Z are also plotted. These will be labelled "pitch" and "yaw" respectively and are denoted by dashed lines in the figure.

The UDS display will show a maximum of four velocities corresponding to pitch and yaw angles measured by each difference amplifier. We expect that corresponding pitch and yaw values will be very close, but the ability to view them simultaneously will provide the integrity checks that are needed.

In addition, the pitch and yaw data described previously will be plotted. Routine operations on the Mission Analysis Computing System (MACS) will involve the generation of ion drift velocity vectors and their graphical presentation as line plots and on polar dials. Figure 4 shows an example of such a display. The three components of ion drift together with additional information available from the RPA and filter banks will be stored in a revised MAF. The displays from these routine operations will be produced on microfilm and microfiche. The displays shown in Figure 4 will also be available from a fully interactive graphics program available to DE investigators.

#### ACKNOWLEDGMENTS

We would like to thank R. F. Bickel for his initial design of the instrument electronics and L. A. Swaim and J. C. Brown for technical support throughout the project.

The hardware effort ongoing and future software efforts are supported by NASA under contracts NAS5-24298, NAS5-26071, NAS5-24297 and NAS5-26068.



References

1. Hoffman, R. A. and Schmerling, E. R.: Space Sci. Instrum. This issue.
2. Schunk, R. W., Banks, P. M. and Raitt, W. J.: J. Geophys. Res., 81,  
3271, (1976)
3. Murphy, J. A., Bailey, G. J. and Moffett, R. J.: J. Atmos. Terr. Phys.,  
38, 351, (1976)
4. Hanson, W. B., Heelis, R. A., Sanatani, S., Lippincott, C. R., Zuccaro,  
D. R., Harmon, L. L., Holt, B. J., Doherty, J. E. and Power, R. A.;  
. Space Sci. Instrum. This issue.
5. Hanson, W. B., Zuccaro, D. R., Lippincott, C. R., and Sanatani, S.;  
Radio Sci.: 8, 333, (1973)
6. Hanson, W. B. and Heelis, R. A., Space Sci. Instrum.: 1, 493, (1975)

FIGURE CAPTIONS

- Fig. 1. A three-dimensional view and 1 dimensional projection of the geometry involved in ion arrival angle measurements by the IDM.
- Fig. 2. Schematic cross-section of the IDM sensor showing the grid configuration and segmented collector.
- Fig. 3. Typical example of expected ion drift velocity output as a function of time along the satellite track. Data from Atmosphere Explorer are used to illustrate the variations that can be expected. Pitch and yaw traces will be identified by different line patterns.
- Fig. 4. Example of refined data display available from geophysical parameters derived from the IDM and RPA. Again Atmosphere Explorer data are used, but better resolution will be available from DE.

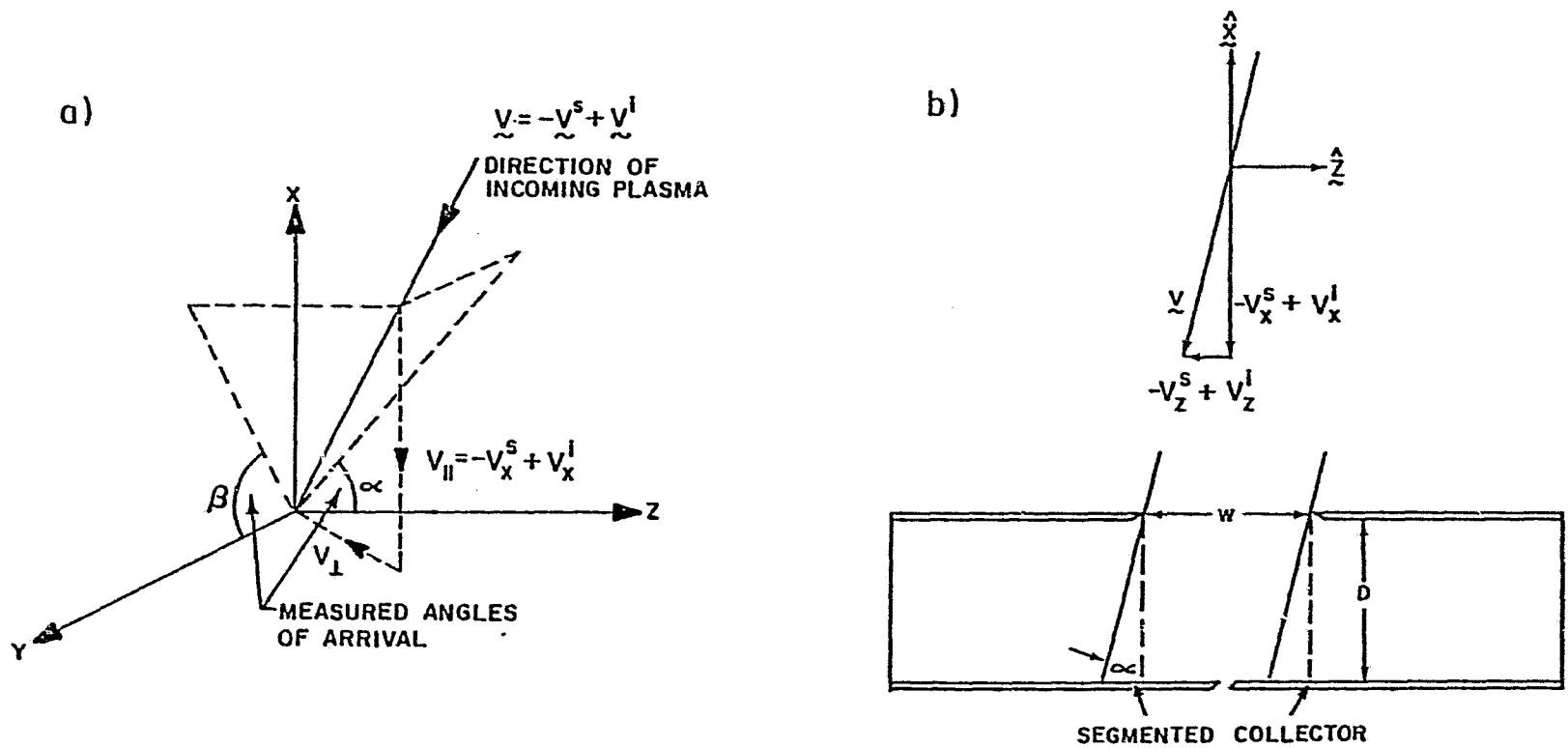
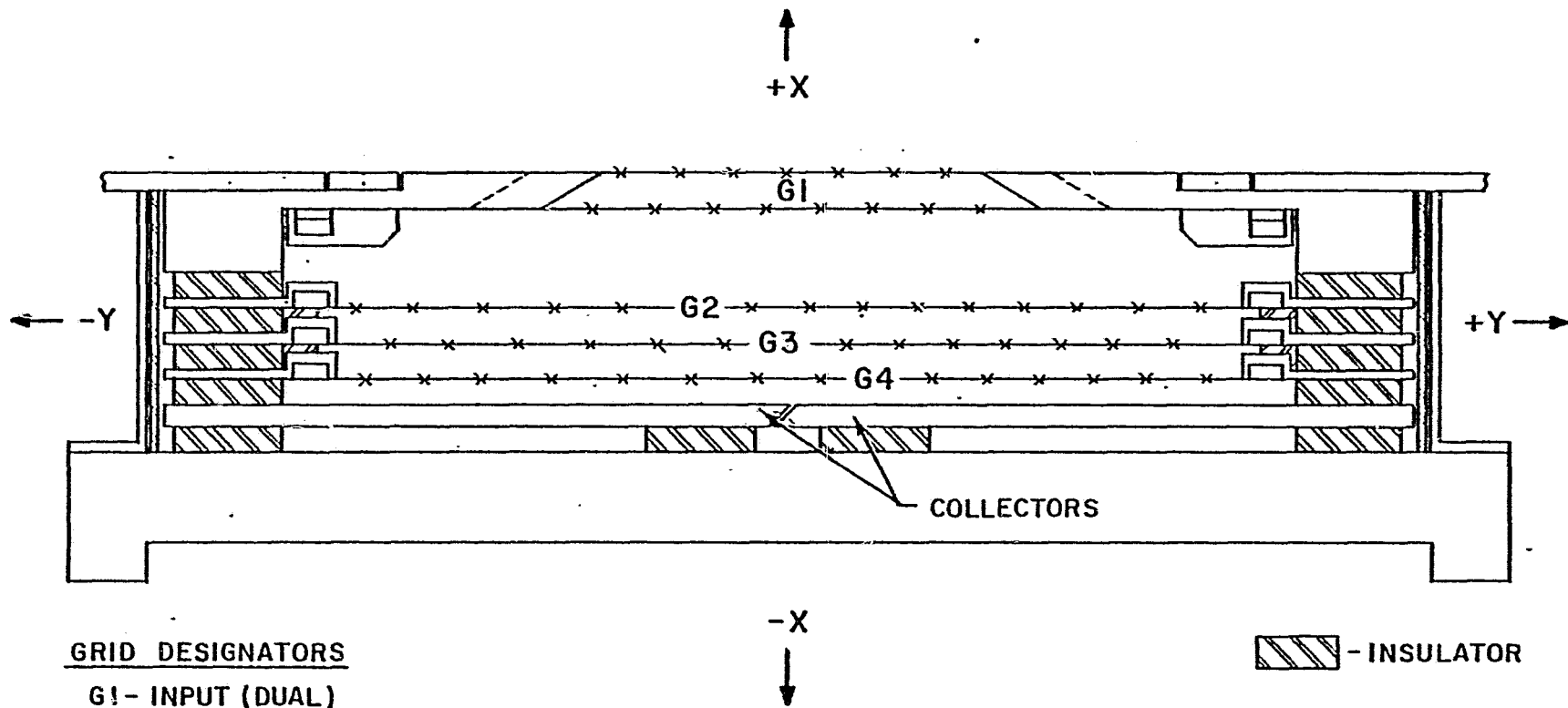


FIGURE 1

ORIGINAL PAGE IS  
OF POOR QUALITY



GRID DESIGNATORS

- G1- INPUT (DUAL)
- G2- SHIELD
- G3- REPELLER
- G4- SUPPRESSOR

 - INSULATOR

**IDM SENSOR CROSS-SECTION**

FIGURE 2

UTD R.A.HEELIS ORBIT 520 • 1 SEPT 81 • UT 8630 SEC • DAY 247 • DE-B • IDM

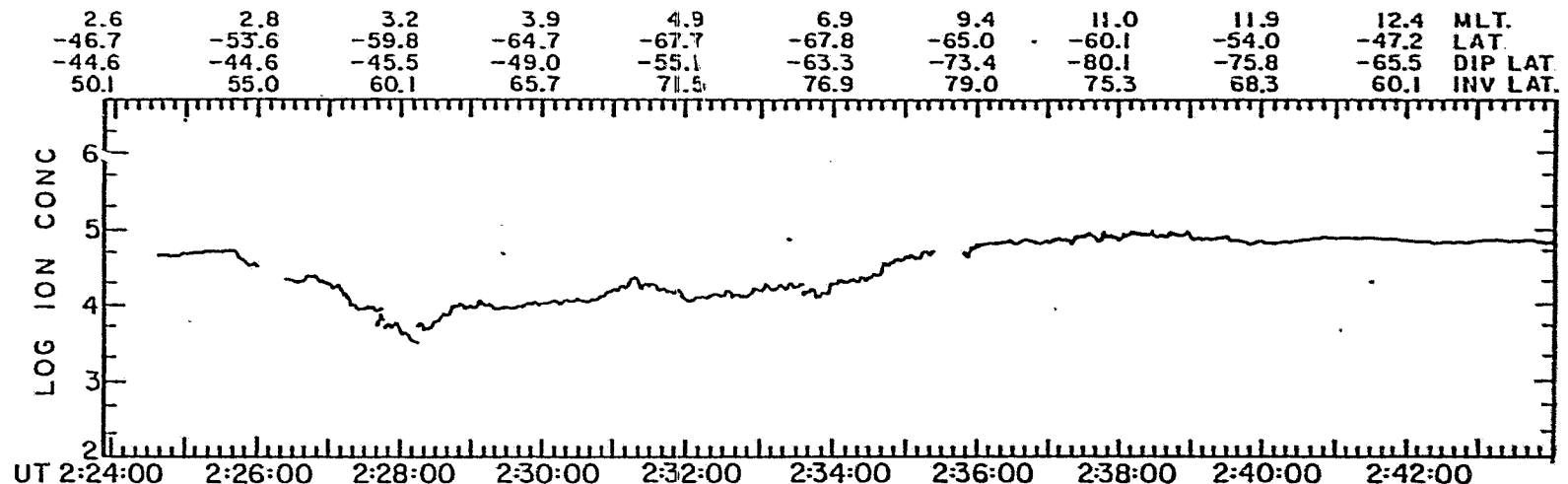
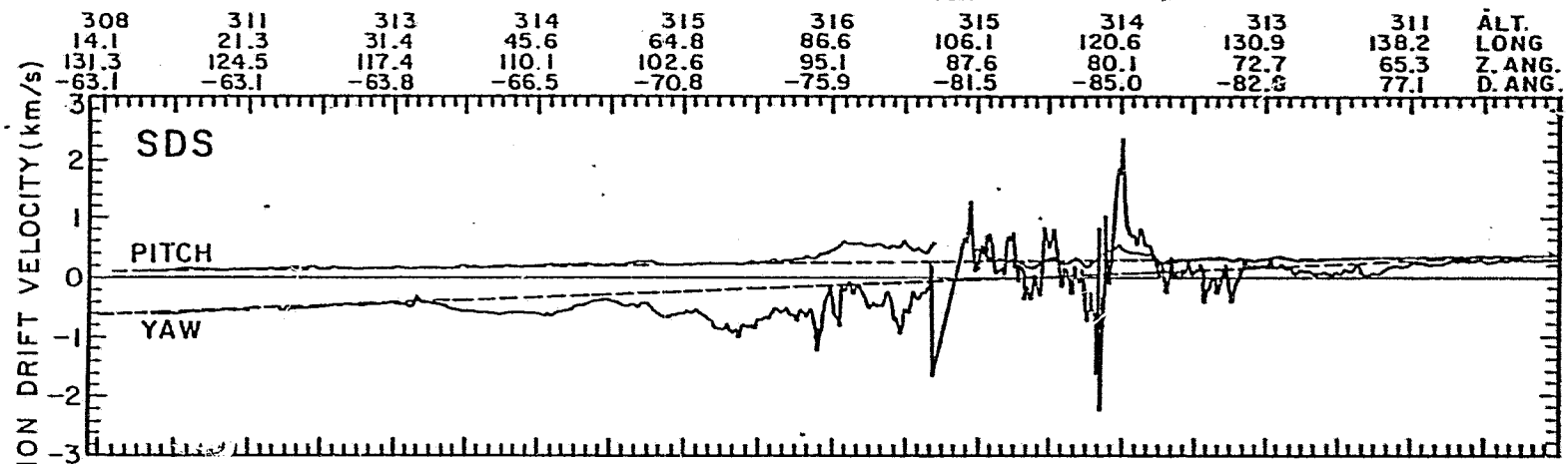
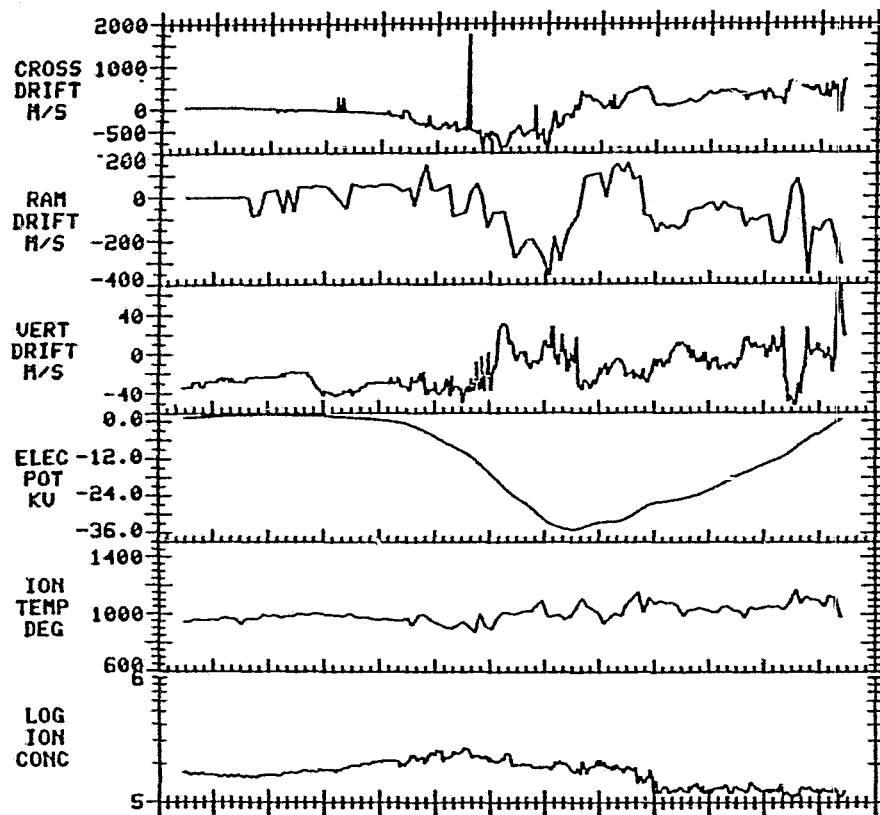


FIGURE 3

ORIGINAL PAGE IS  
OF POOR QUALITY

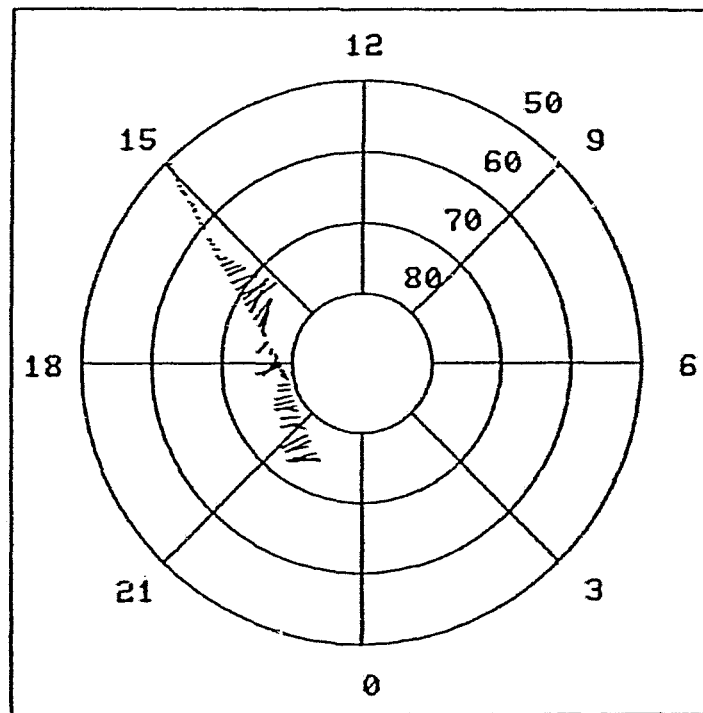
AE-C CONVECTION PARAMETERS  
 DAY-76212 ORBIT-14025 NORTHERN HEMISPHERE



UT (HR:MIN)	1:34	1:37	1:40	1:43
GLAT (DEG)	56.86	64.38	68.03	65.99
GLNG (DEG)	-136.4	-118.2	-90.7	-61.2
MLT (HRS)	15.31	16.16	18.34	22.11
ILAT (DEG)	59.86	70.99	78.86	75.80

UTD SPACE SCIENCES

AE-C ION DRIFT VELOCITIES  
 MLT V ILAT NORTHERN HEMISPHERE  
 DAY 76212 UT 1:40 ORBIT 14025.



1 KM/SEC

FIGURE 4

ORIGINAL PAGE IS  
 OF POOR QUALITY

RETARDING POTENTIAL ANALYZER

FOR

DYNAMICS EXPLORER

FINAL REPORT

For Contract No. NAS5-24298

TO

NATIONAL AERONAUTICS AND SPACE ADMINISTRATION

GODDARD SPACE FLIGHT CENTER

FROM

THE UNIVERSITY OF TEXAS AT DALLAS

CENTER FOR SPACE SCIENCES

W. B. Hanson  
Principal Investigator

R. A. Heelis  
Co-Investigator

C. R. Lippincott  
Co-Investigator

D. R. Zuccaro  
Co-Investigator

FEBRUARY 1982

FINAL REPORT  
CONTRACT NO. NAS5-24298  
RETARDING POTENTIAL ANALYZER  
FOR  
DYNAMICS EXPLORER

SUMMARY

The Retarding Potential Analyzer (RPA) on the Dynamics Explorer B (DE-B) satellite was launched on August 3, 1981, 0956 UT from the Western Test Range. Since turn-on of the instrument, it has performed well and data reduction and analysis have started. Any anomalous instrument operation can be worked around or does not appear to adversely affect the data gathering of the instrument. Long-term data analysis and scientific results will be reported through publication in the appropriate scientific journals. That effort is funded under a separate contract (NAS5-26071) between the University of Texas at Dallas and Goddard Space Flight Center. Other final reports (such as New Technology and equipment) for the hardware contract have been submitted per the contract under separate cover. Also it should be pointed out that all instrument design reviews were completed satisfactorily and all resulting action items closed. Design review data packages were delivered under separate cover at the appropriate time.

It has been demonstrated on Atmosphere Explorer that it is possible to use data from a carefully designed Retarding Potential Analyzer to measure the ram component of the plasma velocity. Since the other two components of the plasma velocity are readily obtainable from an Ion Drift Meter (also flown on AE by UTD), it is thus possible to obtain the complete vector velocity of the bulk plasma motion both along and perpendicular to the magnetic field



in a noninterfering manner, i.e. without the use of booms, antennae, or external electric and magnetic fields.

These techniques have not previously been available, and on A.E. the lack of magnetometers and electric field (AC and DC) instruments has precluded many of the useful correlative studies that can be expected on DE relating to auroral current sheets and other high latitude activity.

This particular investigation defines the thermal structure, bulk motion, and concentration of the thermal ions within the ionosphere and plasmasphere. Knowledge of these parameters, together with others (e.g., particle fluxes, magnetic fields, electric fields, airglow, neutral winds, etc.) that will be measured on the same two spacecraft will allow a very realistic attack to be made on many aspects of the solar wind-atmospheric interaction. The measurements are made with a multigridded planar Retarding Potential Analyzer very similar in concept and geometry to the instruments carried in the current Atmosphere Explorer satellites.

The detailed instrument parameters and investigative approach are presented in the following paper.

THE RETARDING POTENTIAL ANALYZER FOR DYNAMICS EXPLORER-B

by

W. B. Hanson, R. A. Heelis, R. A. Power, C. R. Lippincott,  
D. R. Zuccaro, B. J. Holt, L. H. Harmon and S. Sanatani

Center for Space Sciences  
The University of Texas at Dallas  
Richardson, TX 75080

Accepted by

Space Science Instrumentation

September 1981

## Abstract

The Retarding Potential Analyzer for Dynamics Explorer B measures the bulk ion velocity in the direction of the spacecraft motion, the constituent ion concentrations and the ion temperature along the satellite path. These parameters are derived from a least squares fit to the ion number flux versus energy curve obtained by sweeping or stepping the voltage applied to the internal retarding grids of the RPA. In addition, the spectral characteristics of irregularities in the total ion concentration are determined by high time resolution measurements and by use of a comb filter. These data are obtained from a separate wide aperture sensor.

## INTRODUCTION

The planar retarding potential analyzer (RPA) is a device that measures the energy spectrum of the ambient thermal ions in the vehicle frame of reference on the Dynamics Explorer-B (DE-B) spacecraft. The instrument described here has a lineage that goes back over 20 years. [1],[2],[3] Its predecessors have been flown on several rockets, Air Force satellites, OGO-6, Viking, and Atmosphere Explorers (AE) C, D, and E. Initially the RPA was used to measure the ion concentration ( $N_i$ ) and ion temperature ( $T_i$ ). In satellites it can also sort  $N_i$  into its constituent parts if the various ions present have widely different masses. On OGO-6 a sensitive mode for studying detailed changes in  $N_i$  was introduced [2] that was intended to look for whistler "ducts." Even there, these functions were ascribed to the "duct" mode, though the techniques employed have evolved considerably. Tests with the OGO-6 data also revealed the capability of measuring the bulk ion velocity component normal to the sensor face, and this parameter was routinely derived from the AE data. On AE both the ion characteristic curves and their derivatives were measured since it was anticipated that the latter would be more easily analyzed. [3] On Viking, digital stepping of the retarding potential was employed, rather than a continuous voltage ramp. [4]

In conjunction with the Ion Drift Meter (IDM), also described in this volume [5], the complete bulk ion velocity vector  $\vec{V}_d$  is measured from DE-B. This quantity is fundamental to many of the science objectives of DE at all latitudes. The ion motion affects the ion temperature, both enhancing [6] and diminishing [7] it, and it can also strongly perturb the ion composition at high latitudes [8]. In addition, it has been observed on AE that there is often a strong correlation between  $\vec{V}_d$  and  $N_i$  down to scale sizes of less than 1 km.

Various kinds of plasma instabilities are suspected to be operative in the ionosphere, but to date good evidence for them, particularly at high and mid latitudes, has not been well documented. The combined  $\vec{V}_d$  and  $N_i$  data from DE will cover a large dynamic range in both amplitude and scale size, and it is reasonable to expect that a significant amount will be learned about plasma turbulence, the more so because of the electric and magnetic wave fields also being measured.

#### INSTRUMENT DESCRIPTION

##### A. RPA Sensor Functions

The DE RPA utilizes the planar retarding potential analyzer sensor shown in figure 1, which is oriented with its front face nearly normal to the vehicle velocity vector. Ions entering the aperture in the sensor face pass through a region that is electrically segmented by a series of gold plated tungsten grids before striking the solid collector. The collector ion currents are measured by a linear, automatic ranging electrometer.

The two sensor entrance grids are grounded to the vehicle and surrounded by a conducting ground plane. The next grid inward is the double retarding grid, to which a time-varying electric potential is applied. The suppressor grid is held at a negative potential ( $\sim -15$  volts) to prevent low-energy ambient electrons from reaching the collector and to prevent secondary-electron escape from the collector. The function of the shield grid is to protect the electrometer connected to the collector from the electrical transients generated by changing potentials on the retarding grids; it is also held at vehicle ground. All the grids are woven from 0.025 mm (1 mil) wire, and the number of wires per inch for each grid (in two

perpendicular directions) is indicated in parentheses in the figure.

The retarding potential is variable in the range from approximately +32V to 0V. The details of this voltage trace, and whether it is continuous or stepped, depend on the operating mode of the instrument. The automatic ranging absolute linear electrometer measures the collector current versus retarding voltage, and the derivative of the ion current with respect to retarding voltage can also be measured simultaneously.

The derivative is measured by superposing a small 3400-Hz voltage on the retarding grid voltage. The modulation of the ion current at 3400 Hz, which is proportional to the derivative of the ion current with respect to the retarding grid voltage, is synchronously detected, then amplified and filtered before being presented to the spacecraft data acquisition system. The main electrometer has 8 sensitivity ranges, with adjacent ranges differing in sensitivity by  $10^{1/2}$ , whereas the ranging derivative amplifier has six sensitivity ranges (also with  $10^{1/2}$  sensitivity ratio). During the derivative operation the main electrometer and the derivative amplifier can each be monitored by 2 minor frame analog telemetry words, or all 4 words can be assigned to the derivative amplifier. The sensitivity ranges of the two devices are both monitored with minor frame digital words.

The ion-current characteristics measured in these modes is the primary data transmitted to the ground from the RPA. Subsequently a least-squares fitting technique is used to retrieve the ion temperature, total ion (electron) concentration, information on the composition of major ions, the vehicle potential, and the component of the ion-drift velocity that is parallel to the sensor normal ( $v_d$ ). In essence this velocity component is extracted from the least-squares fitting by finding the mean energy separation between ions of different mass and comparing this energy to that expected from just the vehicle velocity itself.

## B. Duct Sensor Functions

On previous missions we have utilized the same sensor on a time-share basis to measure both the RPA curves and the small scale irregularities in  $N_1$ . A separate sensor is used here for the  $N_1$  measurements to avoid time sharing and to achieve a faster electrometer response by using a larger collecting area. The duct sensor is shown in figure 2. It has approximately 5 times greater effective collecting area than the RPA sensor, and except for the negative electron-suppressor grid all elements are held at spacecraft ground.

The ion current to the collector is measured 64 times per second, approximately every 120 meters of flight path. These measurements can be taken directly from the duct electrometer, or from a difference amplifier that examines changes in the ion current with a 10 times increase in sensitivity. To prevent aliasing, these signals are passed through a three-pole Bessel filter with a 32 hz cutoff before being telemetered.

The ionospheric irregularity measurements are extended to much smaller scale sizes on DE with the aid of a comb filter bank. Six filters are employed, each having a bandwidth of a factor of  $e$  (2.72); their frequency ranges and mean scale sizes are given in Table 1. These filters are connected to a linear wide band amplifier with 5 sensitivity ranges that differ successively by  $10^{\frac{1}{2}}$  in gain. The amplifier sensitivity is controlled by feedback from the filter with the largest output voltage. The filters measure the mean irregularity power within their respective bandwidths

Table 1

Filter Number	1	2	3	4	5	6
Frequency band (hz)	32-86	86-233	233-630	630-1700	1700-4600	4600-12400
Mean scale size (m)	125	46.5	17.2	6.35	2.35	0.87



with about a 45 ms averaging time. Their outputs are sampled every 2 seconds within a period of 375 ms. The wide band amplifier normally monitors the output of the duct electrometer, but every other 2 second period it can be assigned to the difference amplifier output from the Ion Drift Meter.[5] In effect this permits the determination of the irregularity power in the transverse ion drift velocity components at the same scale sizes as those at which  $N_i$  irregularities are being examined.

#### Operations

##### A. RPA Modes

The various RPA modes are differentiated by the manner in which the retarding potential varies with time. This potential can be varied in continuous linear ramps or it can be stepped digitally. In both cases a 3400 hz "wiggle" voltage of selectable amplitude (including zero) is superposed to permit measurement of the derivative of the thermal ion energy spectrum.

Consider first the stepped digital modes. The digital voltages are obtained from an 8 bit digital to analog converter with 10 bit accuracy. The maximum potential of 31.875 volts is divided into 255 equal increments (256 positions) of 125 mv each, and the dwell time per step can be either 16 ms or 32 ms. There is also a digital memory with 256 locations made up of 8 blocks of 32 twelve bit words. The first 8 bits of each word define one of 256 voltage stepper positions and the next three bits define the wiggle amplitude to be superposed. The 8 possible wiggle peak to peak amplitudes are 0, 25 mv, 50 mv, 100 mv, 200 mv, 300 mv, 450 mv, and 600 mv. The twelfth memory word bit selects the output of either the main electrometer or derivative amplifier to be telemetered. This memory can be reloaded in an arbitrary manner by ground command. When the memory is used to control

the retarding grid potential any two of the 8 blocks can be selected to be used alternately. These 64 steps will occur in one second if 16 ms steps are used, or 2 seconds if 32 ms steps are selected. It is anticipated that this will constitute the principal RPA mode of operation.

.. Another mode of digital operation, called the counter mode, has a nearly fixed format with a four-second cycle time. First the ramp voltage is stepped from 31.5 volts to zero in 64 0.5 volt steps with a finite wiggle amplitude. During the next sweep cycle the ramp voltage is stepped from 7.875 volts to zero in 64 0.125 volt steps, again with finite wiggle amplitudes. These two ranges are normally repeated with zero wiggle amplitude. If a 32 ms dwell time is selected, then only the first two ramps occur, but both the electrometer and derivative amplifier will be sampled each step. The 5 basic linear ramp voltage sweeps available to control the retarding grid potential are described in Table 2. All but the first one may be used alone, or the first can be alternated with any of the last four. In addition, the two 12 volt or the two 24 volt ramps can be alternated. The wiggle amplitude can be separately chosen for sweep No. 1 and its alternate.

Table 2

Sweep No.	1	2	3	4	5
Sweep range (volts)	0 + 3	12 + 0	0 + 12	24 + 0	0 + 24
Sweep period (ms)	300	350	350	700	700

## B. Duct Modes

The sampling of changes in the duct sensor ion current is designed to provide higher sensitivity when the ionosphere is smooth than when it is rough. When the ionosphere is rough it is also desirable to have relatively long continuous blocks of data for spectral analysis. This increased sensitivity is achieved in essence by periodically storing the electrometer output voltage at one terminal of a difference amplifier with a gain of 10 X, then connecting the live electrometer to the other difference amplifier terminal. The difference amplifier output is simultaneously set to the midpoint of the 0-5 V analog output so that both positive and negative changes in  $N_1$  can be measured. When  $|\Delta N_1/N_1|$  becomes of the order of 0.1 (depending on the electrometer voltage) the difference amplifier will hit either the upper or lower edge of the output band, at which point the duct electrometer is monitored directly. Enable pulses accompanying each of the RPA words on the subcommutated telemetry frame are used to control the timing of this switching procedure. These enable pulses occur every 2 seconds. If the difference amplifier over-range occurs within 1 second, the words are switched back to the electrometer through the next 8 digital subcom enable pulses (17 to 18 seconds). At the end of this period, they are switched back to the amplifier. If over-range occurs again within 1 second, the words are switched back to the electrometer for another 17 to 18 second period. If over-range does not occur during the 1 second period, one of the two following events will occur:

- a. An amplifier over-range will switch the words to the electrometer and the next digital subcom enable pulse will initiate a new cycle;
- b. After a 16 second period, the words are switched to the electrometer for 1 minor telemetry frame (62.5 ms) and then a new cycle is initiated.

Thus if the ionosphere is relatively smooth, i.e., with  $\Delta N_1/N_1$  of less than a few percent, it will be seen in large blocks of amplifier data. If the ionosphere is rough, then large blocks of duct electrometer data will be taken. At high latitudes the ionosphere is almost always rough by these standards.

As previously described, there is a comb filter bank that samples the irregularity power in  $(\Delta N_1/N_1)$  every two seconds (every four seconds if the filter is being shared with IDM). It will be possible on command transfer to monitor the first 5 filters every 1/4 second.

#### DATA ANALYSIS AND PRESENTATION

It is anticipated that all routine data processing will be performed by programs run on the DE Science Data Processing System at Goddard Space Flight Center. Such large quantities of data can be surveyed most effectively by examining visual data displays, and the data will be plotted on microfiche in several different formats to aid in its digestion. Many of the data, particularly derived parameters, will also be stored on the computer in mission analysis files (MAF's).[9] For checking data validity and for examining small scale phenomena, routine plots will be made of measured ion characteristic curves and their computer fits, as well as of the raw data and spectral analysis of 4 second (and larger) segments of the duct detector data.

Plots of ionospheric parameters will usually be made in 20 minute frames. A routine merging of the ram ion drift velocity component from the RPA with the transverse components from the Ion Drift Meter will take place using data from the mission analysis files. The combined results will be available on the 20 minute time plots as well as in a polar plot format (see IDM description in[5]). The ion temperature, ion constituent concentrations (of  $H^+$ ,  $He^+$ ,  $O^+$  and of molecular ions near perigee), the spacecraft potential, the ram ion drift com-

ponent, and a crude ionospheric roughness parameter will all be plotted together in a 20 minute time frame. In addition, the spectral power of ionospheric irregularities over a range of  $\epsilon^{13}$  in scale size (from less than 1 m to >100 km) will also be plotted in 13 separate spectral bands in 20 minute time frames.

Many specialized plot routines, having some flexibility in parameters plotted (including those available from the MAF files from other instruments) as well as in format, will be utilized on the UTD graphics terminals. This software will be available to other DE investigators with compatible hardware.

#### Acknowledgments

We thank E. R. Schmerling and D. P. Cauffman for their tireless efforts to make the Dynamics Explorer project a reality, and M. Wiskerchen for aiding in the improvement of the computer facilities available. We also thank J. P. McClure for his assistance with the instrument design and L. A. Swain and W. E. Lane for the excellent support they have provided in the construction of the instrument. This work was supported by NASA under contracts NAS5-24298, NAS5-26071, NAS5-24297, and NAS5-26068.

References

- [1] Hanson, W. B. and McKibbin, D. D., J. Geophys. Res., 66, 1667, 1961
- [2] Hanson, W. B., Sanatani, S., Zuccaro, D. R., and Flowerday, T. W.,  
J. Geophys. Res., 75, 5483, 1970
- [3] Hanson, W. B., Zuccaro, D. R., Lippincott, C. R., and Sanatani, S.,  
Radio Sci., 8, 333, 1973
- [4] Hanson, W. B., Sanatani, S., and Zuccaro, D. R., J. Geophys. Res.,  
83, 4351, 1977
- [5] Heelis, R. A., Hanson, W. B., Lippincott, C. R., Zuccaro, D. R.,  
Harmon, L. H., Holt, B. J., Doherty, J. E., and Power, R. A.,  
Space Sci. Instr., this issue, 1981
- [6] Schunk, R. W., Raitt, W. J., and Banks, P. M., J. Geophys. Res., 80,  
3121, 1975
- [7] Hanson, W. B., Nagy, A. F., Moffett, R. J., J. Geophys. Res., 78,  
751, 1973
- [8] Schunk, R. W., Banks, P. M., and Raitt, W. J., J. Geophys. Res., 81,  
3271, 1976
- [9] Smith, P. H., and Freeman, C. H., Space Sci. Instr., this issue, 1981

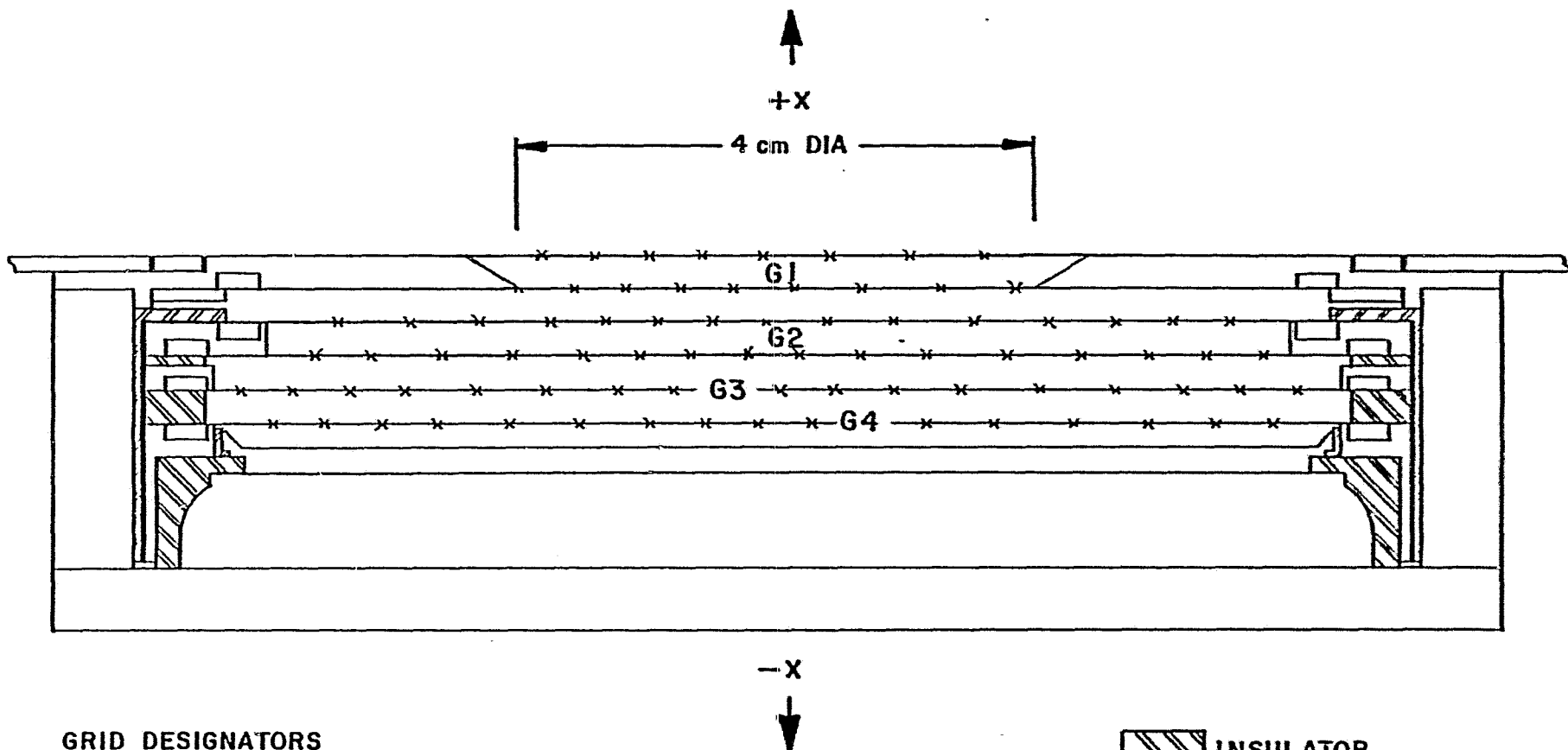
Figure Captions

Figure 1 Schematic cross section of RPA sensor.

All exposed surfaces and inner elements of the RPA sensor, except insulators, are gold plated. The numbers in parenthesis describing the grids give the number of one mil wires per inch. The nominal grid element separation is 2.5 mm.

Figure 2 Schematic cross section of duct sensor.

The duct sensor has the same characteristics as the RPA sensor except for the aperture size and the number of grids.



GRID DESIGNATORS

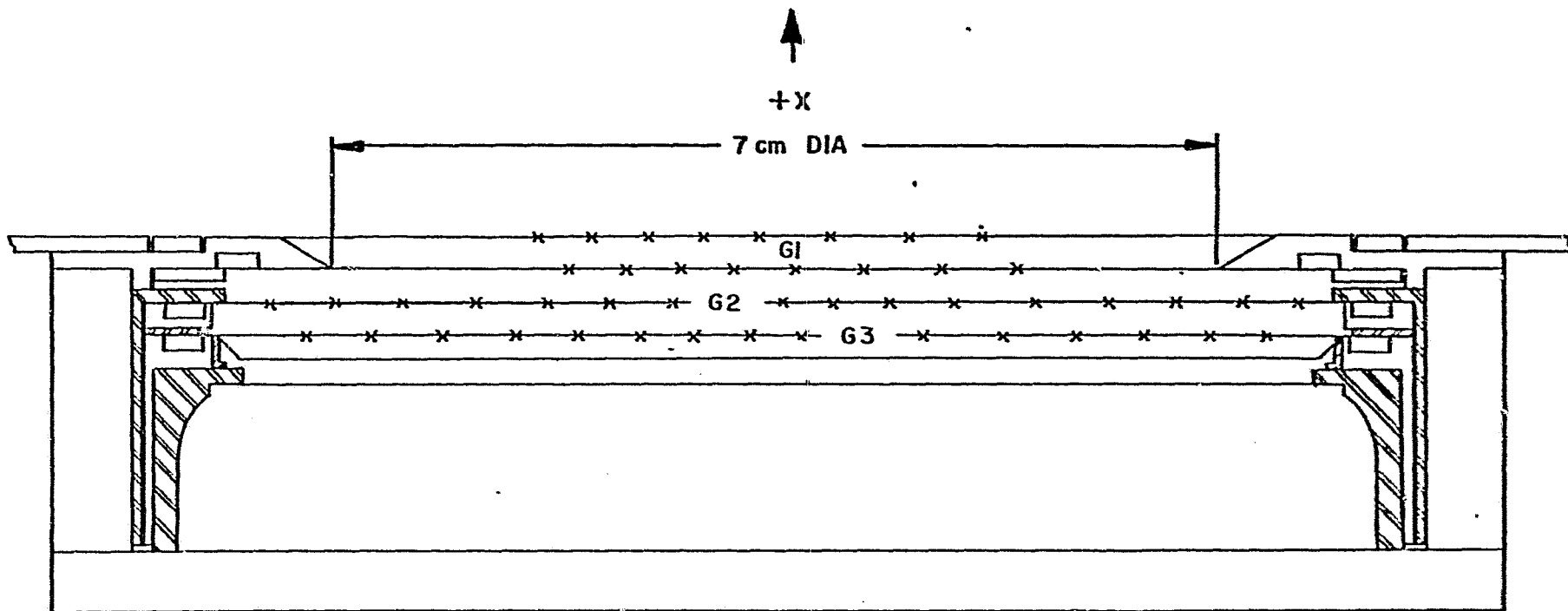
- G1 - INPUT ( DUAL 50/100)
- G2- RETARDING ( DUAL 100/ 50)
- G3- SUPPRESSOR (100)
- G4- SHIELD (50)
- APERTURE -  $12.57 \text{ cm}^2$
- OPTICAL TRANSMISSION = 0.391
- $A_{\text{eff}} = 4.91 \text{ cm}^2$

 INSULATOR

RPA SENSOR CROSS-SECTION

FIGURE I





GRID DESIGNATORS

G1 - INPUT (DUAL)  
 G2 - SUPPRESSOR  
 G3 - SHIELD  
 APERTURE  $\sim 38.5 \text{ cm}^2$   
 OPTICAL TRANSMISSION = 0.663  
 $\cdot A_{\text{eff}} = 25.53 \text{ cm}^2$

(ALL 50 WIRES / INCH,  
 SQUARE GRID MESH)

 INSULATOR

DUCT SENSOR CROSS-SECTION

FIGURE 2